

Modeling of Aerosol Formation during Biomass Combustion in Grate Furnaces and Comparison with Measurements

M. Jöller,* T. Brunner, and I. Obernberger

Institute for Resource Efficient and Sustainable Systems, Research Group “Thermal Biomass Utilisation”, Graz University of Technology, Inffeldgasse 21 B, 8010 Graz, Austria

Received April 16, 2004. Revised Manuscript Received October 27, 2004

Results from mathematical modeling of aerosol formation during combustion of woody biomass fuels were compared with results from particle size distribution (PSD) measurements at a pilot-scale biomass combustion unit with moving grate and flame tube boiler. The mathematical model is a plug flow model considering coagulation, nucleation, condensation, and particle deposition mechanisms (thermophoresis, particle diffusion, turbophoresis, and gravitational settling) of spherical particles as well as condensation of vapors on cooled boiler walls and a changing flue gas composition determined by equilibrium calculations. Additionally, the influence of kinetically limited homogeneous and heterogeneous reactions was taken into account in the case of sulfation reactions. To check the modeling results, investigations regarding PSDs and total aerosol mass loadings of the flue gas resulting from biomass combustion (beech chips, waste wood) were performed by measurements at a fixed bed biomass combustion unit (nominal boiler capacity: 440 kW). Furthermore, the composition of the aerosols sampled was determined. The comparison of calculated and measured particle size distributions and aerosol compositions agreed well, which permits the conclusion to be drawn that the model is applicable to the estimation of amount and chemical composition of aerosol emissions from fixed-bed biomass combustion.

Introduction

The formation of particulate matter in biomass fired heating plants and CHP plants is on one hand a problem in regard to particle emission, especially in small-scale plants with a nominal capacity smaller than 1 MW_{th}, where the installation of efficient aerosol precipitation devices is too expensive to be economic. On the other hand, deposition of particles on furnace and boiler surfaces leads to corrosion and a reduction of the heat transfer, which can cause subsequent plant shutdowns and increased operating costs. But within the scope of advancing biomass combustion for sustainable energy supply, the emissions from biomass combustion devices must be lowered and the efficiency of the combustion units improved. The knowledge of particle formation and deposition mechanisms is important therefore to derive measures for lowering particulate emissions and harmful deposits. Among the particulate matter, aerosols ($d_p < 1 \mu\text{m}$) are of special interest because flue gas cleaning devices show a minimum of precipitation efficiency for particles in the range between 0.01 and 1 μm ,¹ and aerosol forming species have a considerable influence in regard to fouling in heat exchangers.² To examine possible practical influences on aerosol forma-

tion in biomass-fired boilers and to determine amount and chemical composition of particle emissions, an accurate model for aerosol formation and deposition processes in combustion devices is required.

The formation and behavior of aerosols in combustion systems have been studied by several researchers,^{3–10} and their investigations were the basis for further mathematical simulation of aerosol formation and deposition in furnaces and boilers. Mathematical modeling of aerosol formation was initially not only related to the field of combustion but also to industrial processes,¹¹

(3) Kauppinen, E. I.; Pakkanen, T. A. *Environ. Sci. Technol.* **1990**, *24*, 1811–1818.

(4) Quann, R. J.; Neville, M.; Sarofim, A. F. *Combust. Sci. Technol.* **1990**, *74*, 245–256.

(5) Frandsen, F. *Trace Elements from coal Combustion*; Department of Chemical Engineering, Technical University of Denmark: Lyngby, 1995.

(6) Valmari, T.; Kauppinen, E. I.; Kurkela, J.; Jokiniemi, J. K.; Sfiris, G.; Revitzer, H. *J. Aerosol Sci.* **1998**, *29*, 445–459.

(7) Obernberger, I.; Dahl, J.; Brunner, T. In *Proceedings of the 4th Biomass Conference of the Americas on Growth Opportunity in Green Energy and Value-Added Products*, Oakland, CA; Overend, R. P., Chornet, E., Eds.; Pergamon-Elsevier Science Ltd.: Oxford, 1999; pp 1377–1383.

(8) Lind, T. *Ash Formation in Circulating Fluidised Bed Combustion of Coal and Solid Biomass*; Technical Research Centre of Finland (VTT): Espoo, Finland, 1999.

(9) Obernberger, I.; Brunner, T.; Jöller, M. In *Proceedings of the IEA Seminar “Aerosols from Biomass Combustion”*, Zürich, Switzerland; Nussbaumer, T., Ed.; Verenum: Zürich, 2001; pp 69–74.

(10) Brunner, T.; Obernberger, I.; Jöller, M.; Arich, A.; Pölt, P. In *Proceedings of the IEA Seminar “Aerosols from Biomass Combustion”*, Zürich, Switzerland; Nussbaumer, T., Ed.; Verenum: Zürich, 2001; pp 75–80.

(11) Rao, N. P.; McMurry, P. H. *Aerosol Sci. Technol.* **1989**, *11*, 120–132.

* Corresponding author e-mail: joeller@rns.tugraz.at. Fax: +43 (0)-316 481300 4.

(1) Zevenhoven, R.; Kilpinen, P. *Control of Pollutants in Flue Gases and Fuel Gases*; on-line book: <http://www.hut.fi/~rzevenho/gasbook>; 2002.

(2) Nielsen, H. P. *Deposition and High-Temperature Corrosion in Biomass-Fired Boilers*; Department of Chemical Engineering, Technical University of Denmark: Lyngby, 1998.

nuclear technology,^{12,13} atmospheric modeling,^{14,15} and other scientific purposes.^{16,17} The first computer codes dealing with combustion aerosol modeling have been developed for coal and waste combustion^{18–21} because there is a longer tradition of advanced research on coal combustion than on biomass combustion. Concerning aerosol formation from the combustion of biomass fuels, Christensen²² predicted aerosol formation in straw combustion units by the Plug Flow Aerosol Condenser. Recent modeling work focusing on biomass combustion combined aerosol formation codes with computational fluid dynamics (CFD).^{23,24}

Aerosol formation during biomass combustion is only partially comparable with aerosol formation during coal combustion because the chemical composition, the release behavior, and the combustion temperatures are different in biomass and coal furnaces. Investigations of fly ash particle formation during fixed-bed combustion of European woody biomass fuels (namely, chemically untreated wood chips, bark, and waste wood) were performed by Obernberger et al.⁹ It was ascertained that fly ashes can be divided into a coarse part ($d_p > 1 \mu\text{m}$) containing mainly Ca, Mg, Si, K, and Al and a submicron part (the aerosols) of which the chemical composition greatly varies with the chemical composition of the fuel used. Furthermore, the formation pathway of the aerosols is expected to be different for the fuel types investigated.

It was shown that for chemically untreated wood chips ash-forming matter released from the fuel bed consists to a great amount of K, S, and Cl forming gaseous compounds, which undergo nucleation and subsequent condensation on particle surfaces. The presence of a relevant amount of seed particles influencing aerosol formation can be ruled out definitively due to chemical analyses of aerosol size fractions, which show the most important seed particle compound for wood chips (namely, Ca) to be mainly present in the coarse particle fraction. Ca compounds are not expected to become gaseous under conditions present during biomass combustion, as chemical equilibrium calculations have shown.

During the combustion of bark considerable amounts of submicron Ca-rich particles, which act as seed

particles for the condensation of alkali sulfates and chlorides, are released directly from the fuel bed along with the elements mentioned for wood chips. These particles may act as seeds for condensation; therefore, nucleation rates of new particles might be decreased. The concentration of Ca in the aerosol fractions from bark combustion is thus clearly higher than from combustion of chemically untreated wood chips. Additionally, the content of heavy metals in the fuel and the aerosols is higher than from chemically untreated wood chips but does not have a strong influence on aerosol formation.

Furthermore, particle formation during the combustion of waste wood is also different. The main aerosol-forming elements are Na, K, Cl, S, Zn, and Pb. Based on thermodynamic data of Zn compounds, Zn is expected to evaporate in the reducing atmosphere of the fuel bed to subsequently form ZnO, which nucleates forming seed particles for all further condensable species. Nucleation of considerable amounts of further aerosols seems to be suppressed by surface condensation on these ZnO particles. This is confirmed by the fact that the distribution of the Zn concentration in the aerosol fractions from waste wood combustion follows the particle size distribution and Zn seems to be present in most aerosol size fractions.

Previous modeling approaches of aerosol formation during combustion were often restricted to the formation of aerosols either from alkali metal species or from heavy metal species and to a limited number of different seed particle size classes. The modeling approach presented in this paper includes data for modeling aerosol formation from both groups of species, as this is required for simulating the formation of aerosols from the combustion of waste wood, which contains relevant amounts of alkali metals as well as heavy metals.⁹

To check the simulation results concerning particle size distributions (PSD) and chemical composition of the particles formed, measurements with a Berner-type low-pressure impactor (BLPI) were performed at a pilot-scale combustion unit. Then, the particles sampled were analyzed by means of wet chemical analyses in order to determine the chemical composition of the sampled aerosol fractions. This procedure should provide evidence of the degree of applicability of the modeling approach.

Model Description

General Modeling Approach and Model Setup.

The aerosol formation model was set up as a plug flow model including the particle formation mechanisms of nucleation, condensation, and agglomeration as well as particle deposition (thermophoresis, particle diffusion, turbophoresis, and gravitational settling) and vapor condensation on furnace and boiler surfaces. The model is one-dimensional, which implies that no resolution of the gas volume perpendicular to the flue gas channel is made and that gradients of gas and particle properties in the bulk gas stream are neglected. But data representing the boundary conditions (such as diameters, perimeters, and temperatures of the combustion unit sections) are used, and relevant transport mechanisms are treated with wall functions.

The gas-phase composition, which is the basis for modeling particle formation processes, is determined by

(12) Im, K. H.; Ahluwalia, R. K.; Chuang, C. F. *Aerosol Sci. Technol.* **1985**, *4*, 125–140.

(13) Williams, M. M. R. *Prog. Nucl. Energy* **1996**, *30*, 333–416.

(14) Wilck, M. *Modal Modelling of Multicomponent Aerosols*; VWF Verlag für Wissenschaft und Forschung: Berlin, 1999.

(15) Warren, D. R.; Seinfeld, J. H. *Aerosol Sci. Technol.* **1985**, *4*, 31–43.

(16) Gelbard, F.; Seinfeld, J. H. *J. Comput. Phys.* **1978**, *28*, 357–375.

(17) Gelbard, F.; Tambour, Y.; Seinfeld, J. H. *J. Colloid Interface Sci.* **1980**, *76*, 541–556.

(18) Lin, W. Y.; Sethi, V.; Biswas, P. *Aerosol Sci. Technol.* **1992**, *17*, 119–133.

(19) Lin, W. Y.; Biswas, P. *Combust. Sci. Technol.* **1994**, *101*, 29–43.

(20) Jokiniemi, J. K.; Lazaridis, M.; Lehtinen, K. E.; Kauppinen, E. *J. Aerosol Sci.* **1994**, *25*, 429–446.

(21) Lockwood, F. C.; Yousif, S. *Fuel Process. Technol.* **2000**, *65*–66, 439–457.

(22) Christensen, K. A. *The Formation of Submicron Particles from the Combustion of Straw*; Department of Chemical Engineering, Technical University of Denmark: Lyngby, 1995.

(23) Kær, S. K. *Numerical Investigation of Deposit Formation in Straw-Fired Boilers*; Institute of Energy Technology, Aalborg University: Aalborg, Denmark, 2001.

(24) Pyykönen, J. *Computational Simulation of Aerosol Behaviour*; VTT Processes, Processes and Environment: Espoo, Finland, 2002.

chemical equilibrium calculations. Kinetically limited gas-phase reactions are considered by introduction of an Arrhenius approach. Then the particle formation and deposition processes are calculated. After each of the calculation steps, particle and gas properties are adapted to the new conditions.

The aerosol formation model was restricted to the formation of particles of compounds that are stable under oxidizing flue gas conditions. Thus the starting point of the calculations was set to the secondary air inlet of the combustion plant, because the assumption was made that at the point of secondary air inlet the flue gas is burned out and oxidizing flue gas atmosphere prevails. Therefore, initial conditions for the simulation are given by the initial flue gas properties such as temperature, pressure, gas composition, and the primary particle size distribution at this point.

In the modeling approach presented, the possibility of inserting primary particles in various sizes, amounts, and various chemical compositions allowed the requirements for modeling aerosol formation from different biomass fuels to be considered. Primary particles are already present at the calculation starting point and are mostly raised from the fuel bed by the gas stream. During their residence time in the flue gas, they may undergo changes due to aerosol formation processes and chemical reactions with the surrounding flue gas, and finally they may deposit on furnace and boiler walls. The coarse primary fly ash particles from the combustion of woody biomass consist mainly of compounds, which have low volatility under the given conditions such as CaO or SiO₂ and of not released amounts of volatile compounds such as compounds of potassium and sulfur. Regarding the aerosols, the amount of primary particles may vary greatly depending on the kind of biomass fuel used.

In addition to the initial conditions, boundary conditions are required, which are flue gas and wall temperature, pressure, gas velocity, and the residence time in the calculation volume. Flue gas temperature and pressure along the gas stream were interpolated from single measurement values, and concerning the wall temperatures the assumption was made that the temperature is about 100 °C in the boiler regions (boiler and fire tube) and about 50–100 °C below the average flue gas temperature in the furnace. Gas velocity and residence time were calculated from the volume flow at the respective temperature, pressure, and geometric data of the combustion plant.

The required data for initial and boundary conditions as well as data for the comparison of measured and calculated aerosol properties were gained from test runs performed with selected biomass fuels and from element mass balances based on these tests. The mass balances provided the amount of matter released from the fuel bed, and subsequent thermodynamic equilibrium calculations allowed estimating the mass of ash forming matter in the gas phase and in primary particles.

The calculation results are the total mass of aerosol particles, the aerosol PSD, the chemical composition of aerosol particles, and the flue gas composition at the boiler outlet.

Chemical Composition of Gas Phase and Particles. Detailed knowledge about the gas phase com-

position is essential for the simulation of the aerosol formation process because the amount of the relevant gas phase compounds greatly affects mass, chemical composition, and size distribution of the particles formed. The actual composition of the gas phase is therefore determined at the beginning of each calculation step by performing a thermodynamic equilibrium calculation. Solid and liquid phases are excluded from the calculation of the condensable compounds in order to achieve possible supersaturations, which are needed to calculate gas to particle conversion processes. For integrating the equilibrium calculations into the calculation procedure, the commercial package Chemsheet was used. The compilation of the relevant thermodynamic data was performed with FactSage.

Regarding the particle composition, chlorides and sulfates of alkali and earth alkaline metals are expected to be dominant. Additionally, for chemically untreated woody biomass fuels, the amounts of alkali metals, especially potassium, exceed the sum of chlorine and sulfur to such an extent that the formation of alkali carbonates is highly probable.²² Therefore, in the present approach thermodynamic data of gaseous potassium carbonate (K₂CO₃) were also used, although also a heterogeneous formation of K₂CO₃ is supposed to occur.²⁵

Furthermore, the formation of gaseous sulfur compounds is known to be kinetically limited at flue gas temperatures below approximately 820 °C.²⁶ To implement the kinetic limitation in the current approach by an Arrhenius equation as done by Christensen et al.,²⁷ the oxidation reaction of SO₂ to SO₃ was set as the limiting step assuming that for the formation of gaseous sulfates the presence of SO₃ is required. The SO₃ formed was taken as sulfur input for a second thermodynamic equilibrium calculation in each control volume, which was used to determine the amounts of alkali sulfates in the gas phase. To fit the modeling results of SO₂/SO₃ in the gas phase to measured values, the parameters of the Arrhenius equation were adapted for each modeling case.

Heterogeneous reactions between gas and particles, especially sulfation reactions, may have a further impact on the gas-phase and particle compositions. In the step-by-step calculations these reactions are not considered, but the possible effect on particle and gas composition is considered while estimating the amounts of primary particles.

To guarantee the applicability of the thermodynamic gas-phase calculation model, the most stable compounds of the following elements from woody biomass fuels were evaluated by test calculations: H, C, N, O, S, Cl, F, P, Si, Na, Mg, K, Ca, Al, Fe, Cu, Zn, Pb, Cd, and Hg.

Gas to Particle Conversion Processes. Gas to particle conversion occurs when compounds in the flue gas become supersaturated due to cooling or expansion of the gas or as a result of chemical reactions. This change of state of aggregation can either occur by

(25) Steinberg, M.; Schofield, K. *Combust. Flame* **2002**, *129*, 453–470.

(26) Livbjerg, H. In *Proceedings of the IEA Seminar "Aerosols from Biomass Combustion"*, Zürich, Switzerland; Nussbaumer, T., Ed.; Verenum: Zürich, pp 29–30.

(27) Christensen, K. A.; Stenholm, M.; Livbjerg, H. *J. Aerosol Sci.* **1998**, *29*, 421–444.

heterogeneous condensation and nucleation of vapors on existing surfaces or by homogeneous nucleation.

For the latter process, homogeneous nucleation, Becker and Döring²⁸ derived the classical model of nucleation, which was later extended by several authors.^{29–32} The modeling approach developed by Ford et al.³¹ was used for the calculation of the nucleation rate in this aerosol formation model. Nucleation starts with the random formation of small molecule clusters, which can either grow or evaporate until they have reached a critical radius (r^*). Then they become stable and will only grow further. At the critical cluster radius the partial pressure (p_i) of the vapor equals the saturation vapor pressure ($p_{i,S}$) at the surface of the clusters. This point is strongly affected by the surface tension of the nucleating species, which itself is again affected by the particle size. This effect is expressed by the so-called Tolman relation (including Tolman length, τ). According to this relation, the surface tension of a KCl particle with a diameter of 0.01 μm is expected to be about 5% smaller than without considering this effect (data taken from Christensen²²). But because of a serious lack of Tolman length data for most of the condensable species and possible validity limitations of the Tolman relation,³³ this effect was not considered in the simulations.

The other way vapors can transform into a liquid or solid phase is condensation/nucleation on existing surfaces, which is on particles in the flue gas, respectively. In this modeling approach heterogeneous condensation only was used. An equation expressing the molecular rate of condensation $F_{i,j}$ of species i on N_j particles of size $d_{p,j}$ in the control volume for the entire range of the particle size was derived by Fuchs and Sutugin³⁴ (eq 1):

$$F_{i,j} = 2\pi D_i d_{p,j} N_j \frac{p_i - p_{i,S}}{R_{\text{gas}} T} C_{FS} \quad (1)$$

D_i and C_{FS} in eq 1 are the diffusion coefficient and the Fuchs–Sutugin correction factor, respectively. In the aerosol formation model, eq 1 was used for the calculation of the rates of condensation of different condensable compounds on the different particle classes. The condensable species considered in the calculations performed were K_2SO_4 , KCl , K_2CO_3 , Na_2SO_4 , NaCl , ZnCl_2 , PbO , and PbCl_2 and the dimers $(\text{KCl})_2$ and $(\text{NaCl})_2$.

Coagulation of Particles. While gas to particle conversion processes change the total amount of solid and liquid phases, this mass remains constant during the process of coagulation, which effects only the PSD. Collisions between the particles occur due to the different motions of the aerosol particles relative to each other. Subsequently these particles then may adhere to

each other or coalesce. In this model coagulation is treated as coalescence, and the particles are always treated as absolute spheres.

Causes for the relative motion of the particles can either be Brownian motion (thermal coagulation) or external forces (kinematic coagulation).³⁵ The change in the particle size distribution caused by coagulation mechanisms is determined with collision frequency functions, which represent coagulation probabilities and are calculated separately for each mechanism.

For the mechanism of Brownian motion a formula for the collision frequency derived by Fuchs³⁶ was used. Important coagulation mechanisms caused by external forces considered in the aerosol modeling code are gravitational settling and turbulent shear. The collision frequency function of gravitational settling is calculated according to Hinds.³⁵ Turbulent eddies also cause relative motion of particles and subsequent coagulation. The expression used for the calculation of the collision frequency function caused by turbulent eddies is given by Saffman and Turner.³⁷

Furthermore, the single coagulation frequency functions are summed up and multiplied with the actual size class particle numbers (N_i , N_j) to obtain the effective number of collisions of two particle classes i and j per unit time and volume.

Particle and Vapor Deposition. A part of the entrained and the newly formed particles in the flue gas deposits on furnace and boiler walls together with vapor condensation of aerosol forming compounds. These processes may cause slag formation in furnace regions and a reduction of the heat transfer as well as corrosion in the boiler section.

The main mechanisms in combustion devices that lead to particle deposition are gravitational settling, inertial impaction, particle diffusion, and thermophoresis. Since the model is a one-dimensional plug flow reactor model and no impaction of large particles on tube banks had to be considered, the effect of inertial impaction was skipped. This is in fact of minor relevance for aerosol particles but has an influence on the deposition modeling for coarse fly ash particles.

Particle and vapor deposition processes always occur together with erosion, shedding, and re-entrainment of particles, which play an important role for the build-up of deposits. In the plug flow model these deposit build-up processes must be considered by a general re-entrainment factor for each particle size and location in the plant.

Gravitational Settling. Gravity is one of the external forces causing particle movement and subsequent deposition, but for turbulent tube flow it is only relevant for coarse particles. To calculate the amount of settled particles the so-called terminal settling velocity is determined with the particle Reynolds number (Re_p), which expresses the relation of viscous effects and inertial effects during particle motion. Relations for the determination of the settling velocity ($v_{\text{dep,settle}}$) at different Reynolds numbers are reported by Hinds.³⁵ For the determination of the amount of settled particles in

(28) Becker, R.; Döring, W. *Ann. Phys.* **1935**, *24*, 719–752.

(29) Girshick, S. L.; Chiu, C.-P. *J. Chem. Phys.* **1990**, *93*, 1273–1277.

(30) Girshick, S. L.; Chiu, C.-P.; McMurry, P. H. *Aerosol Sci. Technol.* **1990**, *13*, 465–477.

(31) Ford, I. J.; Barrett, J. C.; Lazaridis, M. *J. Aerosol Sci.* **1993**, *24*, 581–588.

(32) Dillman, A.; Meier, G. E. A. *Chem. Phys. Lett.* **1989**, *160*, 71–74.

(33) Koga, K.; Zeng, X. C.; Shchekin, A. K. *J. Chem. Phys.* **1998**, *109*, 4063–4070.

(34) Fuchs, N. A.; Sutugin, A. G. In *Topics in Current Aerosol Research*; Hidy, G. M., Brock, J. R., Eds.; Pergamon Press: New York, 1971; pp 1–60.

(35) Hinds, W. C. *Aerosol Technology*, 2nd ed.; John Wiley and Sons Inc.: New York, 1999.

(36) Fuchs, N. A. *The Mechanics of Aerosols*; Dover Publications Inc.: New York, 1964.

(37) Saffman, P.; Turner, J. J. *J. Fluid Mech.* **1956**, *1*, 16–30.

combustion applications, the approach of stirred settling was used.³⁸

Deposition by Thermophoresis. Particles exposed to a temperature gradient in the surrounding gas will be drawn into the direction of decreasing temperature, which is called thermophoresis.

In this modeling approach, the following relation (eq 2) for the thermophoretic velocity ($v_{\text{dep,th}}$) was used. The factor K_{th} is the thermophoretic coefficient by Talbot et al.,³⁹ which is valid for the whole particle size range. The validity range of the equation was the reason for preferring it to other relations:

$$v_{\text{dep,th}} = \frac{-\eta_{\text{gas}} K_{\text{th}} \Delta T}{\rho_{\text{gas}} T} \quad (2)$$

Deposition by Particle Diffusion and Turbulent Eddies. In a particle-laden gas stream, a gradient of the particle concentration will always be established at boundary walls because unlike gas molecules the particles do not rebound from the walls.³⁵ For the determination of the amount of particles deposited by diffusion from turbulent flow with a plug flow approach, it is commonly assumed that in the turbulent bulk stream the concentration of particles is uniform and in the boundary layer the concentration decreases linearly to zero at the wall. Turbulent eddies of the gas stream additionally contribute to particle deposition by throwing particles toward the wall, which was mainly relevant for coarse particles under the given conditions in the boiler ($\text{Re} < 30000$, $v_{\text{gas}} < 25\text{m/s}$).

In this model, the special case of deposition during tube flow is taken as an approach for particle removal by diffusion and turbulent eddies. The particle number decrease during the flow through a tube of length l and diameter d_t was calculated with the following expression (eq 3)³⁵ using a deposition velocity (v_{dep}), which considers both mechanisms, diffusion, and turbulent impaction:⁴⁰

$$N = N_0 \exp\left(\frac{-4v_{\text{dep}}l}{d_t v_{\text{gas}}}\right) \quad (3)$$

Vapor Condensation at Boundary Walls. In addition to particle formation and deposition processes, direct condensation of aerosol-forming species on furnace and boiler walls also occurs. This mechanism is considered with the approach for condensation of vapor mixtures in the presence of inert gases according to VDI.⁴¹

Determination of the Primary Particle Composition. Taking into account the influence of primary particles on aerosol formation, coarse primary particles and primary aerosols must be considered separately. Especially primary aerosols will act as seed particles for precipitation of condensable matter. Furthermore, during particle formation the coarse particles will remain virtually unchanged while the chemical composition as well as the PSD of the aerosols will change significantly.

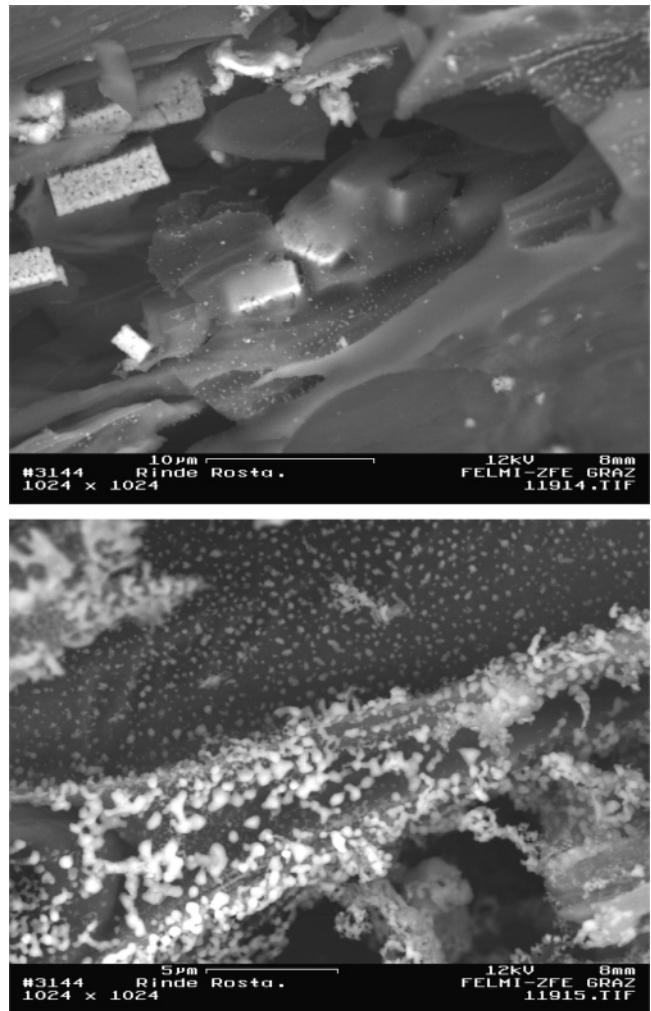


Figure 1. SEM images of charcoal particles from biomass combustion; samples taken from partly unburned fuel particles from the grate of a biomass combustion unit firing bark; first: Ca-containing crystals formerly consisting of calcium oxalate are set free by combustion, second: Ca-containing particles (also submicron) are driven out of the charcoal; analyses performed at the Institute of Electron Microscopy, Graz University of Technology.

With respect to aerosol formation from woody biomass, the main elements in fly ash particles forming low volatility compounds are, according to their thermodynamic data, Ca, Mg, Si, and Zn.¹⁰ In woody biomass (e.g., spruce), calcium is present mainly as oxalate and in water-soluble form.⁴² Under furnace conditions, calcium oxalate decomposes first to calcium carbonate (CaCO_3) and later on to calcium oxide (CaO). To check the occurrence of Ca in the fuel during combustion of woody biomass, investigations on charcoal particles were performed by means of scanning electron microscopy (SEM)/energy-dispersive X-ray spectrometry (EDX) analyses (Figure 1).

The investigations confirmed previous results,^{9,10} which showed coarse particles containing most of the Ca in supermicron crystals and chain agglomerates as well as in aerosol particles formed with Ca seeds.

In the presence of SO_2 , CaO reacts to CaSO_4 and CaSO_3 .⁴³ A simulation of the reaction process requires

(38) Davies, C. N. In *Aerosol Science*; Davies, C. N., Ed.; Academic Press: London, 1966; pp 393–446.

(39) Talbot, L.; Cheng, R. K.; Schefer, R. W.; Willis, D. R. *J. Fluid Mech.* **1980**, *101*, 737–785.

(40) Lee, K. W.; Gieseke, J. A. *J. Aerosol Sci.* **1994**, *25*, 699–709.

(41) VDI. *Wärmeatlas*, 8th ed.; Springer: Berlin, 1997.

(42) Marschner, H. *Mineral Nutrition of Higher Plants*, 2nd ed.; Academic Press: San Diego, 1995.

data about the CaO structure. Specific surface and pore size distributions are properties that may differ considerably and have a considerable influence on the reaction progress, since after pore plugging has occurred, the reaction is limited by product layer diffusion. Literature data about the structure of CaO from calcium oxalate formed by combustion of biomass could not be discovered by the authors. Therefore, and because of the short residence time of aerosol particles in the calculation compared to experiments, the possible amount of CaO conversion was determined with the CaO conversion values of Adánez et al.,⁴⁴ which do not exceed approximately 15% for a residence time of 2 s.

Mg compounds are expected to behave in a manner similar to Ca compounds, but the concentration of Mg is much lower than that of Ca; therefore, the possible effects on the flue gas and gas composition were neglected.

In waste wood also Si is present in greater amounts⁹ mainly because of cullet, but with only a few exceptions Si is assumed to be present mainly in coarse fly ash particles. Furthermore, Si is not expected to undergo rapid reactions with considerable quantities of aerosol-forming species. No reactions of Si were thus considered in the model.

The fate of Zn in combustion systems has already been explained in the Introduction. It mainly forms ZnO, which subsequently nucleates to aerosol particles. ZnO particles are therefore not primary particles entrained from the fuel bed, but they are assumed to be present when further condensable compounds become supersaturated and convert to particles.

Mathematical Description and Numerical Solution. A general mathematical description of aerosol formation and transport processes of particles of different size classes in a control volume has been given by the General Dynamic Equation (GDE):⁴⁵

$$\frac{\partial N_j}{\partial t} + (\nabla N_j v_{\text{gas}}) = \nabla D_{p,j} \nabla N_j - \left(\frac{\partial N_j}{\partial t} \right)_{\text{growth}} + \left(\frac{\partial N_j}{\partial t} \right)_{\text{coag}} + (\nabla N_j v_p) \quad (4)$$

In this equation the change of the number of particles in size class j with time in a control volume is determined by the source and sink terms for particle coagulation, particle growth, homogeneous nucleation, vapor condensation, particle diffusion into and out of the control volume, particle motion due to the gas velocity (v_{gas}), and due to the relative velocity v_p of the particles. v_p is caused by external forces such as gravity and thermophoresis and, together with particle diffusion, may lead to particle deposition.

Furthermore, in this modeling approach the particle size distribution is represented by the so-called “nodal point method”.²⁰ With this method, the particle size distribution (PSD) is treated as a discrete size distribution, whereas the sections are reduced to their mean diameters. New particles with a diameter between two

sectional mean diameters, resulting particle formation processes, are allocated to the two already existing classes. This kind of representation of the PSD conserves the mass and number of particles in the gas. The number of size classes must be adapted to the modeling problem in order to achieve results of sufficient accuracy. In this study the number of size classes was set to 100 with diameters equally logarithmically distributed between 10^{-3} and $500 \mu\text{m}$.

Additionally, beside the aerosol population balance, a balance of the gas-phase components was implemented. The set of equations to be solved covers therefore balancing equations for j particle classes and for i and k condensable and noncondensable compounds, respectively. The system was solved by spatial discretisation into the flow direction, whereas during one calculation step the operation conditions were assumed to be quasi-stationary. Then, in each modeled control volume, first the gas composition was determined. The particle formation and deposition processes were not calculated in the following as a set of equations but in random sequence and finally, at the end of each calculation step the balances were updated. The whole model was developed as VBA-Code using MS Excel for data input and output.

Experimental Section

To check the applicability of the aerosol formation model, calculations were performed, and the results were compared with measured particle size distributions obtained from test runs with woody biomass fuels at a fixed-bed combustion plant. Within these test runs, each of which lasted 48 h, fuel as well as ash and gas samples (bottom ash, boiler fly ash fractions, total suspended particles, SO_2/HCl samples) were taken regularly in order to perform chemical analyses and to determine the mass flows of fuel and ashes. Operating data were recorded during the test run period and evaluated. This information provided the basis for balances of the relevant elements over the combustion plant. Furthermore, the initial and boundary conditions chosen in these test calculations were gained from these analyses.

Description of the Biomass Combustion Plant. The plant consists of a furnace with a horizontally moving grate, staged primary air inlet, a secondary combustion zone, and a flame tube boiler consisting of a fire tube and two ducts of flame tubes. Combustion temperatures can be controlled by flue gas recirculation below and above the grate. The nominal boiler capacity amounts to $440 \text{ kW}_{\text{th}}$. A scheme of the combustion unit is given in Figure 2.

Measurement Techniques. The PSD measurements at the boiler outlet were performed with a nine-stage Berner-type low-pressure impactor (BLPI) and an upstream nozzle for isokinetic sampling. The BLPI was heated before and during the sampling period in order to avoid condensation of water on the sample foils.

Measurements of the total amount of suspended particles in the flue gas at the boiler outlet were performed according to VDI-2066. The sampling of HCl and SO_x from the flue gas was performed by sucking a defined, dust-free flue gas stream through a set of bottles filled with $\text{H}_2\text{O}/\text{H}_2\text{O}_2$. Furthermore, the total amounts of ashes were sampled for balancing and samples for wet chemical analyses were taken at periodic intervals. To obtain information about the chemical composition of aerosols sampled on the impactor stages, wet chemical analyses regarding the elements Ca, Si, Mg, Na, K, S, Cl, Zn, and Pb were performed.

(43) Marsh, D. W.; Ulrichson, D. L. *Chem. Eng. Sci.* **1985**, *40*, 423–433.

(44) Adánez, J.; García-Labiano, F.; Fierro, V. *Chem. Eng. Sci.* **2000**, *55*, 3665–3683.

(45) Friedlander, S. K. *Smoke Dust and Haze*; John Wiley & Sons: New York, 1977.

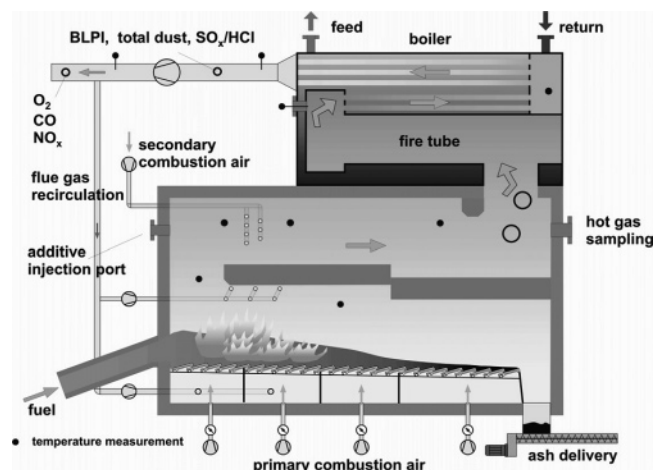


Figure 2. Scheme of the biomass combustion plant used for ash sampling and for particle size distribution measurements of aerosols; BLPI, Berner low-pressure impactor.

Table 1. Composition of the Biomass Fuels Investigated in Regard to Aerosol-Forming Elements

element	fuel [mg/kg d.b.] ^a		element	fuel [mg/kg d.b.] ^a	
	beech	waste wood		beech	waste wood
S	134	621	Ca	2236	5008
Cl	40.0	585	Fe	95.5	1305
Si	<400	2811	Cu	1.6	14.7
Na	12.0	466	Zn	7.4	238
Mg	328	761	Pb	0.63	83.6
K	1209	919	Cd	0.05	0.61

^a d.b., dry basis.

Results from Test Runs and Model Input

Fuel Composition. Chemically untreated wood chips and waste wood were chosen as fuels for this study. As can be seen from the wet chemical analysis results in Table 1, the concentrations of aerosol-forming species in waste wood are clearly higher than in chemically untreated wood chips except for K. Also, the ratios of S and Cl content to the alkali content of the fuels differ, which should be relevant for the aerosol composition.

Mass Concentration and PSD of Aerosol Particles. The BLPI measurements performed during the test runs yielded the following averaged results, which were taken as a reference for comparison with aerosol formation calculations.

Several impactor measurements were performed during the combustion of beech and waste wood. Plant operation data such as temperatures, flue gas volume stream, energy output, and oxygen content in moist and dry flue gas were recorded simultaneously. The evaluation of the data showed that the average emissions of submicron particles at the boiler outlet were 46.6 and 68.5 mg/Nm³ (related to 13 vol % O₂ in dry flue gas) for beech and waste wood, respectively. The mean particle size distributions of combustion aerosols from beech and waste wood are shown in Figure 3. It can clearly be seen that the peak of the PSD from beech combustion is situated on the 3rd stage (cut diameter: 0.125 μm) whereas for aerosols from waste wood combustion the peak is partly on the 3rd and the 4th stage (cut diameter: 0.25 μm). During the combustion of waste wood under the same conditions of residence time and temperature and in the same time, a higher mass of

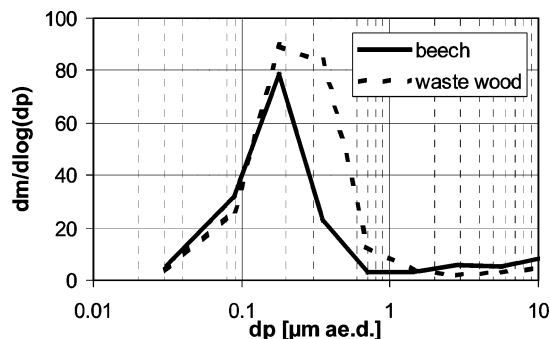


Figure 3. Mean particle size distributions measured at the boiler outlet; measurements performed with a 9-stage Berner-type low-pressure impactor (BLPI); values in mg/Nm³ 13 vol % O₂ dry gas; ae.d., aerodynamic diameter; the first stage represents the final particle filter.

Table 2. Amounts of Elements Considered for Aerosol Formation Simulation at the Calculation Starting Point in the Flue Gas

element	fuel [mol/mol]		element	fuel [mol/mol]	
	beech	waste wood		beech	waste wood
H	1.04E-01	1.04E-01	Mg	4.28E-06	2.74E-06
C	3.97E-02	3.97E-02	K	1.10E-05	7.31E-06
N	6.39E-01	6.38E-01	Ca	8.93E-06	1.79E-05
O	2.18E-01	2.17E-01	Fe	1.56E-05	1.79E-04
S	4.06E-06	7.24E-06	Cu	1.28E-08	1.07E-07
Cl	1.16E-06	1.32E-05	Zn	8.21E-08	8.18E-06
Si	1.66E-06	1.20E-05	Pb	2.00E-09	4.83E-07
Na	9.79E-07	5.83E-06	Cd	5.07E-10	4.08E-09

aerosol-forming matter is distributed in the flue gas (Table 2). Compared to aerosols from beech combustion this produces bigger particles, which form mainly because of stronger coagulation.⁴⁵

Chemical Composition of Aerosol Particles. Results of the analyses of BLPI samples taken during beech combustion are shown in Figure 4.

It can clearly be seen that K and S are enriched in the finer particles, which are mainly formed by gas to particle conversion. On the other hand, the amount of Ca and Mg increases with the particle diameter. Cl, Na, and Zn concentrations follow no clear trend, which can be related to the low concentration of these elements. Furthermore, as can be seen in Figure 3, the impactor stages with a cut diameter above 1 μm show very low sampled mass as compared to the smaller stages. This implies higher uncertainties of the results obtained for these stages.

Results of wet chemical analyses of aerosol particles from waste wood combustion are plotted in Figure 5. The concentrations of the elements K, Cl, Na, and Pb show a tendency to decrease with increasing particle diameter, whereas the amount of Ca increases with increasing particle diameter. S shows a weak tendency to be enriched in the bigger particles and the Zn concentration follows the particle size distribution (i.e., the Zn concentration is highest for size fractions with the highest mass).

Input Data for Particle Formation Modeling. The evaluation of the test run operating data of the combustion unit, which included temperatures, thermal output of the plant, gas composition, and flue gas velocity at the boiler outlet, allowed the compilation of plant profiles for temperature, pressure, flue

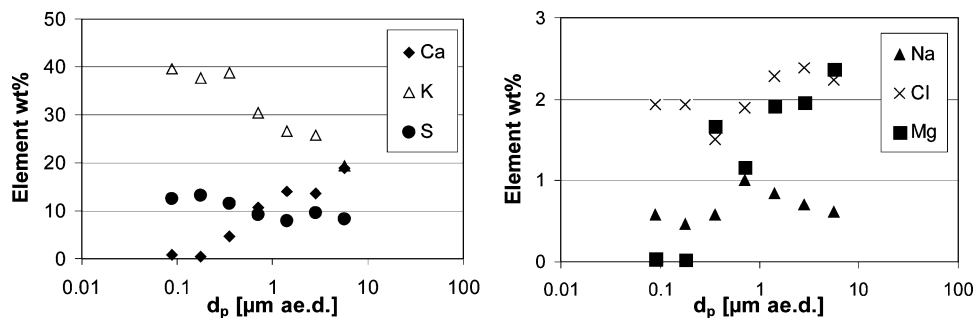


Figure 4. Concentrations of aerosol forming compounds in particles sampled on impactor plates during beech combustion; ae.d., aerodynamic diameter; elements considered exceed 1 wt % at any stage; results normalized to 100%.

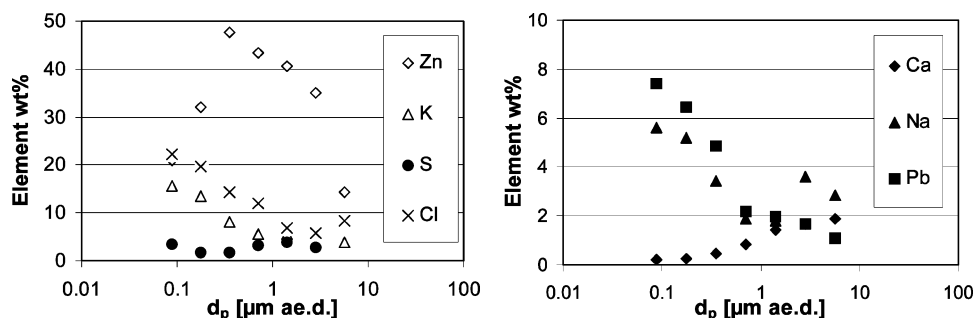


Figure 5. Concentrations of aerosol forming compounds in particles sampled on impactor plates during waste wood combustion; ae.d., aerodynamic diameter, elements considered exceed 1 wt % at any stage; results normalized to 100%.

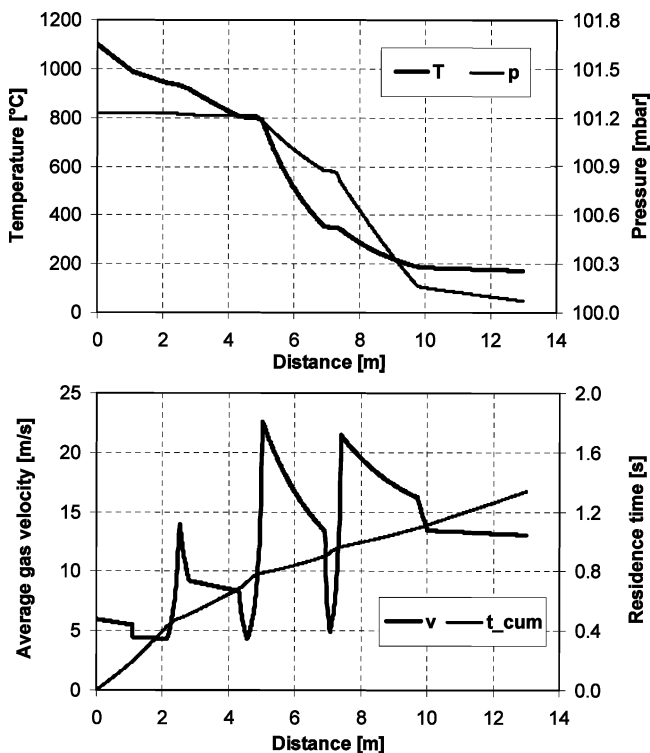


Figure 6. Characteristic plant data vs. the distance in the plant; T , temperature; p , pressure; v , gas velocity; t_{cum} , residence time cumulated from the secondary air inlet to the relative distance; 0 m, secondary air inlet.

gas velocities, and residence times (Figure 6) as described in the General Modeling Approach and Model Setup.

Gas temperature, pressure, and geometric data of the plant at the calculation starting point served as initial conditions. Further initial conditions for the simulation

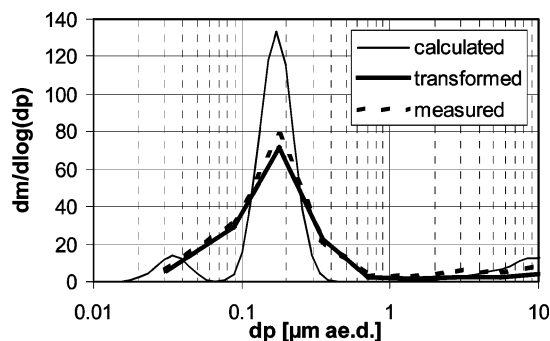


Figure 7. Simulated and measured particle size distributions of aerosols from beech combustion at the boiler outlet; calculated, calculated particle size distribution; transformed, particle size distribution transformed to virtually measured PSD; measured, averaged measured PSD.

calculations were particle and gas properties in the hot furnace. In Table 2, the amounts of elements leaving the fuel bed are listed for chemically untreated wood and waste wood.

From these data, the amounts of nonvolatile compounds were estimated by means of chemical equilibrium calculations at the local gas temperatures (between 900 and 1200 °C) as described in chapter the General Modeling Approach and Model Setup. These calculations indicated the following stable compounds: CaSO_4 , CaO , MgO , SiO_2 , K_2SO_4 , ZnO , Na_2CO_3 , and K_2CO_3 . CaSO_4 , CaO , MgO , and SiO_2 were supposed to be released as solids and therefore considered totally as primary particles. The possible amount of CaSO_4 formed was determined as explained in Determination of the Primary Particle Composition. Furthermore, the other compounds obtained were assumed to be partially solid and partially gaseous.

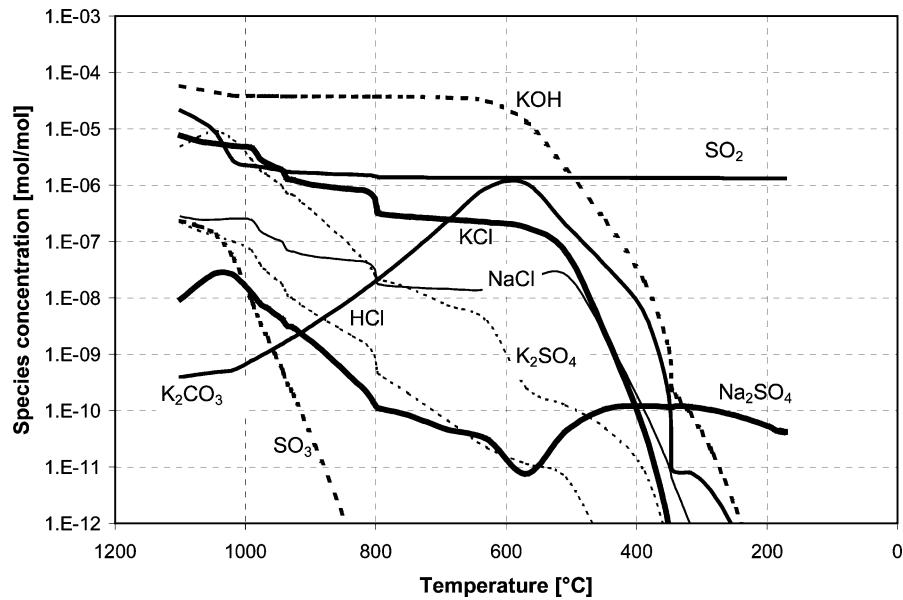


Figure 8. Calculated gas-phase concentrations of species relevant for aerosol formation during beech combustion; initial element concentrations are given in Table 2.

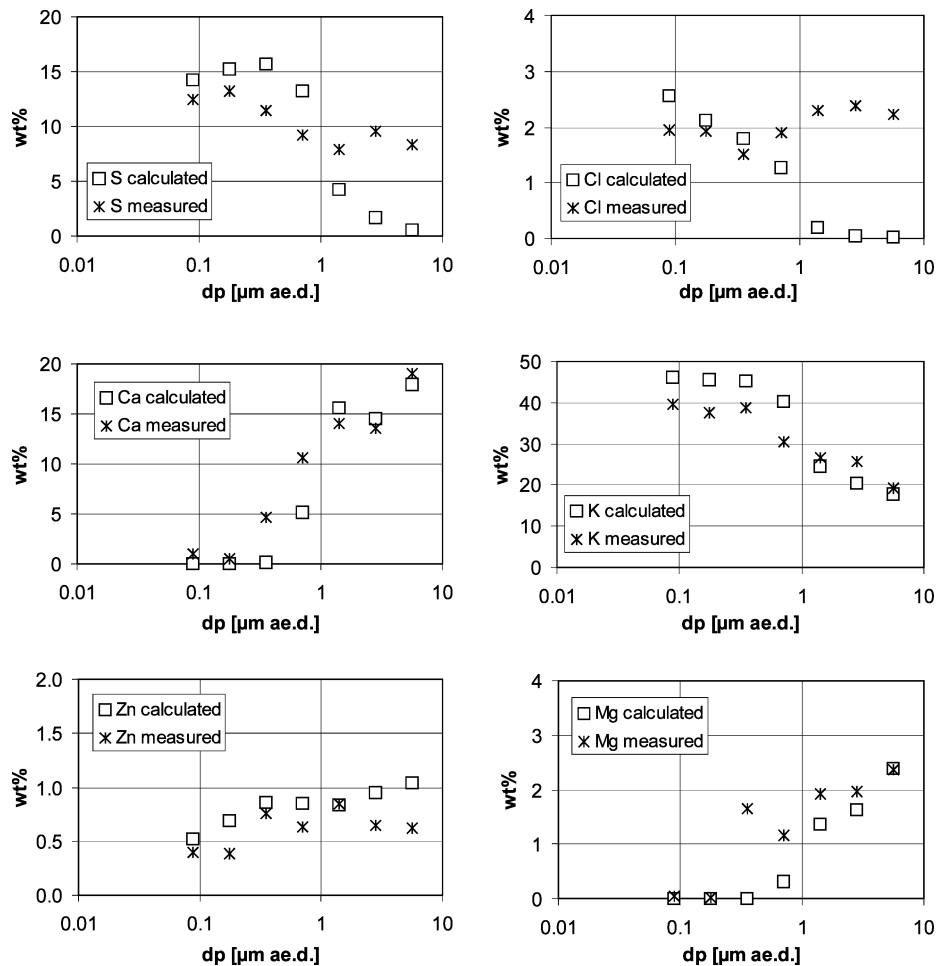


Figure 9. Comparison of simulated and measured concentrations of aerosol forming compounds sampled on impactor plates at the boiler outlet during beech combustion; ae.d., aerodynamic diameter.

The PSD of coarse particles was modeled with measured fly ash size distributions at the boiler outlet from the test runs performed. For the submicron particles a suitable particle mode had to be found by the test calculations.

Results from Modeling Calculations

Adaptations Required for the Comparison of Calculated and Measured PSDs. To be able to compare calculated and measured PSDs, the calculated

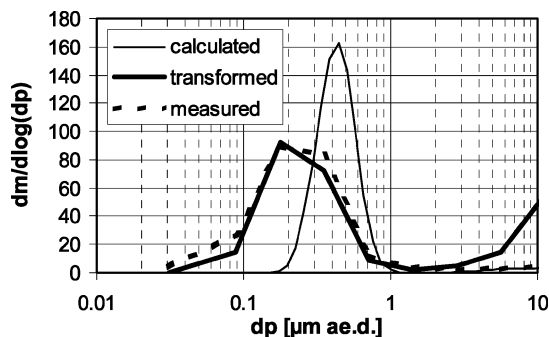


Figure 10. Simulated and measured particle size distributions of aerosols from waste wood combustion at the boiler outlet; calculated, calculated particle size distribution; transformed, particle size distribution transformed to virtually measured PSD; measured, averaged measured PSD.

PSD has to be transformed by determining the mass of particles precipitated on the impactor stages. This is done for each calculated particle size class by use of a precipitation efficiency function (η_{pr}) in terms of the impactor stage cut diameter d_{50} and the particle diameter d_p ⁴⁶ (eq 5):

$$\eta_{pr} = \frac{e^{A_{pr} \cdot \ln(d_p/d_{50})}}{1 + e^{A_{pr} \cdot \ln(d_p/d_{50})}} \quad (5)$$

The procedure is applied to all impactor stages beginning at the one with the largest cut diameter, and it gives both the particle size distribution and the average chemical composition of the calculated impactor stages.

Results from Simulating Aerosol Formation from Beech Combustion. Figure 7 shows the mass size distributions of the aerosol fraction for the measured, the calculated, and the transformed case. The calculated PSD consists of two peaks located at about 0.02 and 0.15 μm .

The transformation of the calculated PSD into a value as obtained from a nine-stage BLPI resulted in a PSD with the main peak on the 3rd stage at a cut diameter of 0.125 μm . The second, smaller peak was in the range of the final filter of the BLPI. This result was obtained when the size of the primary aerosols used in the calculations was set around 0.02 μm . Smaller primary aerosols ($\sim 0.01 \mu\text{m}$) resulted in a shift of the main peak to the 2nd impactor stage and larger primary aerosols ($\sim 0.05 \mu\text{m}$) caused a larger mean diameter. These distributions show good agreement with the measured PSD, whereas the main peak is a little smaller. A possible reason for this effect is that particle deposition may be overpredicted in the calculations.

The calculated total mass of particles with an aerodynamic diameter smaller than 1 μm was about 42 mg/Nm³ (related to 13 vol % O₂ and dry gas). The average mass of aerosols measured was 46.6 mg/Nm³ (related to 13 vol % O₂ and dry gas). One main reason for the difference is probably the simplification of the calculation model to a plug flow model, which cannot consider changing temperature and concentration gradients perpendicular to the gas flow. Moreover, the fact that the deposition calculations are performed for clean tubes and boiler walls in contrast with the measurements,

where fouling has occurred, may also influence the results.

In Figure 8, the calculated concentrations of relevant aerosol-forming compounds from beech combustion in each control volume are plotted versus the flue gas temperature. During the calculations the first condensable K compound, which became stable as a condensed phase, was K₂SO₄ followed by KCl. When the concentrations of S and Cl compounds in the flue gas had decreased and hydroxides were stable in appropriate amounts, KCl precipitation was followed by formation of considerable amounts of K₂CO₃ particles. K₂CO₃ formed a second peak of particles with a mean diameter smaller than 0.1 μm under the given time–temperature profile (see Figure 7). NaCl was the first condensable Na compound to become stable followed by Na₂SO₄. Zn, and Pb compounds played no major role for aerosol formation from the combustion of beech.

The point of beginning kinetic limitation of SO₂ oxidation had to be adapted to the modeling problem in the way that the Arrhenius parameters had to be set in the way that the final SO₂ concentration reached values comparable to the measured values, which were about 2 mg/Nm³ related to 13 vol % O₂ and dry gas. A variation of this kinetic limitation may have a powerful affect on the concentration of sulfates in the aerosols formed. In contrast to SO₂ the concentration of HCl, of which the formation is not supposed to be kinetically limited, decreases continuously to values below 10⁻¹⁰ mol/mol. The measured values for HCl emissions during beech combustion were about 0.5 mg/Nm³ (related to 13 vol % O₂ and dry gas) (about 5 · 10⁻⁷ mol/mol), which indicates a possible limitation of HCl reactions in the gas phase.

Figure 9 shows calculated and measured concentrations of the major aerosol forming elements in fractionated aerosol particles from beech combustion (K, Na, Ca, Mg, S, and Cl). Generally, for the aerosol particles the calculation results show the same tendencies as the measurement results. The concentrations of K and S decrease with increasing particle diameter while the concentrations of Ca increase with increasing particle diameter. The varying concentration trends of Na and Cl were reproduced especially for the smallest particles. The composition of particles with a diameter > 1 μm is on one hand greatly affected by the predefined, averaged chemical composition of the primary particles. On the other hand, the surface of a real coarse particle may be much larger than that of the simulated sphere. Therefore in this size range condensation and coagulation are probably underpredicted, and simulated composition values differ from measured ones.

Results from Simulating Aerosol Formation during Waste Wood Combustion. Measured and calculated mass size distribution results of aerosols from waste wood combustion are shown in Figure 10. The calculated PSD forms one peak with a mean particle size between 0.4 and 0.5 μm .

The transformed calculated and measured PSDs have their peak on the 3rd and 4th stage of a nine-stage BLPI at cut diameters 0.125 and 0.25 μm , respectively. Furthermore, the peaks show good compliance regarding total amount and shape. As in the calculation for beech combustion, the primary particles had to be

(46) Kröpfl, P.; Berner, A.; Reischl, G. P. *J. Aerosol Sci.* **2003**, Suppl. 2, 1239–1240.

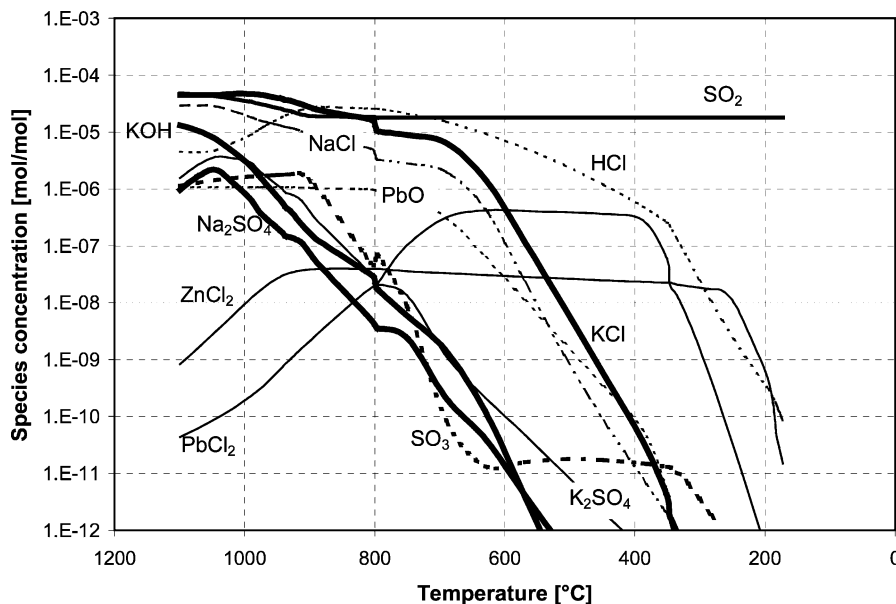


Figure 11. Calculated gas-phase concentrations of species relevant for aerosol formation during waste wood combustion; initial element concentrations are given in Table 2.

introduced at a certain size relative to their amount, which in this case was around $0.08 \mu\text{m}$. A slight difference between the calculated and measured PSDs was determined, which can be explained by the lower mass of aerosols obtained from the calculations (see next paragraph). In contrast to the results for beech combustion, no second peak formed, probably because enough surface for condensation of aerosol forming species was provided.

The mass of aerosol particles obtained from the calculations was 62.7 mg/Nm^3 , which is lower than the average measured concentration of 68.5 mg/Nm^3 (both related to 13 vol % O_2 and dry gas). As in the calculation with beech as fuel, the simplified model and the assumption of clean boiler tubes are assumed to be responsible for the differences.

In Figure 11 the calculated amounts of gaseous species relevant for aerosol formation during waste wood combustion are shown. The first compound undergoing gas to particle conversion was Na_2SO_4 followed by K_2SO_4 , KCl , NaCl , PbO , PbCl_2 , and finally ZnCl_2 . This order is confirmed by the thermodynamic properties of the substances, which indicate that, in the concentration ranges considered, condensed alkali sulfates are already stable at higher temperatures than alkali chlorides, which are again stable at higher temperatures than heavy metal compounds. Enough S and Cl were provided to form K_2SO_4 and KCl but not K_2CO_3 , which is not stable in this case according to thermodynamic data. Furthermore, the oxide was the most stable product of Pb at temperatures above 600°C , while below that temperature PbCl_2 predominated. Finally, ZnCl_2 , the only condensable compound of Zn considered, became condensed below 300°C .

As for the beech combustion, the temperature of the beginning kinetic limitation of SO_2 oxidation was adapted to the modeling problem. By this means an SO_x concentration of about 20 mg/Nm^3 related to 13 vol % O_2 and dry gas was reached, which is in the range of the averaged measured value (22 mg/Nm^3 related to 13 vol % O_2 and dry gas). The final concentration of HCl in

the flue gas was too low compared with the measured values (approximately 0.8 mg/Nm^3 related to 13 vol % O_2 and dry gas), as it has been the case for beech combustion.

Comparisons of calculated and measured element concentrations of aerosol fractions are plotted in Figure 12. Generally the trends were reproduced: K, Na, Cl, and Pb show decreasing concentration with increasing particle diameter, while S and Ca show increasing concentrations with increasing particle diameter. The Zn concentration is highest in the aerosol fraction with the highest mass loading. The total concentrations, however, could not be reproduced in all cases. They differ especially for coarse particles, where the small mass loadings of the analyzed samples lead to uncertain concentration values and the simulation of condensation and coagulation may be underpredicted. In the aerosol range for Zn the sharp peak observable in the measurements did not form in the calculations. The reasons are probably a fluctuation of element release compared to the averaged values from the element balances and missing data concerning PSD and composition of primary particles.

Conclusions

A plug flow model was developed in order to simulate aerosol formation during the combustion of different woody biomass fuels including waste wood. The model includes the determination of the gas phase composition by means of thermodynamic equilibrium calculations and kinetically limited sulfation reactions. For this purpose, calculations of the rate of SO_2 to SO_3 conversion as the limiting step were implemented by an Arrhenius expression. The particle formation mechanisms included are homogeneous nucleation, heterogeneous condensation, and coagulation. Furthermore, thermophoresis, diffusion from turbulent duct flow, gravitational settling, and wall condensation of vapors were considered in order to determine the amount of deposited aerosol particles and condensable matter at furnace and boiler walls.

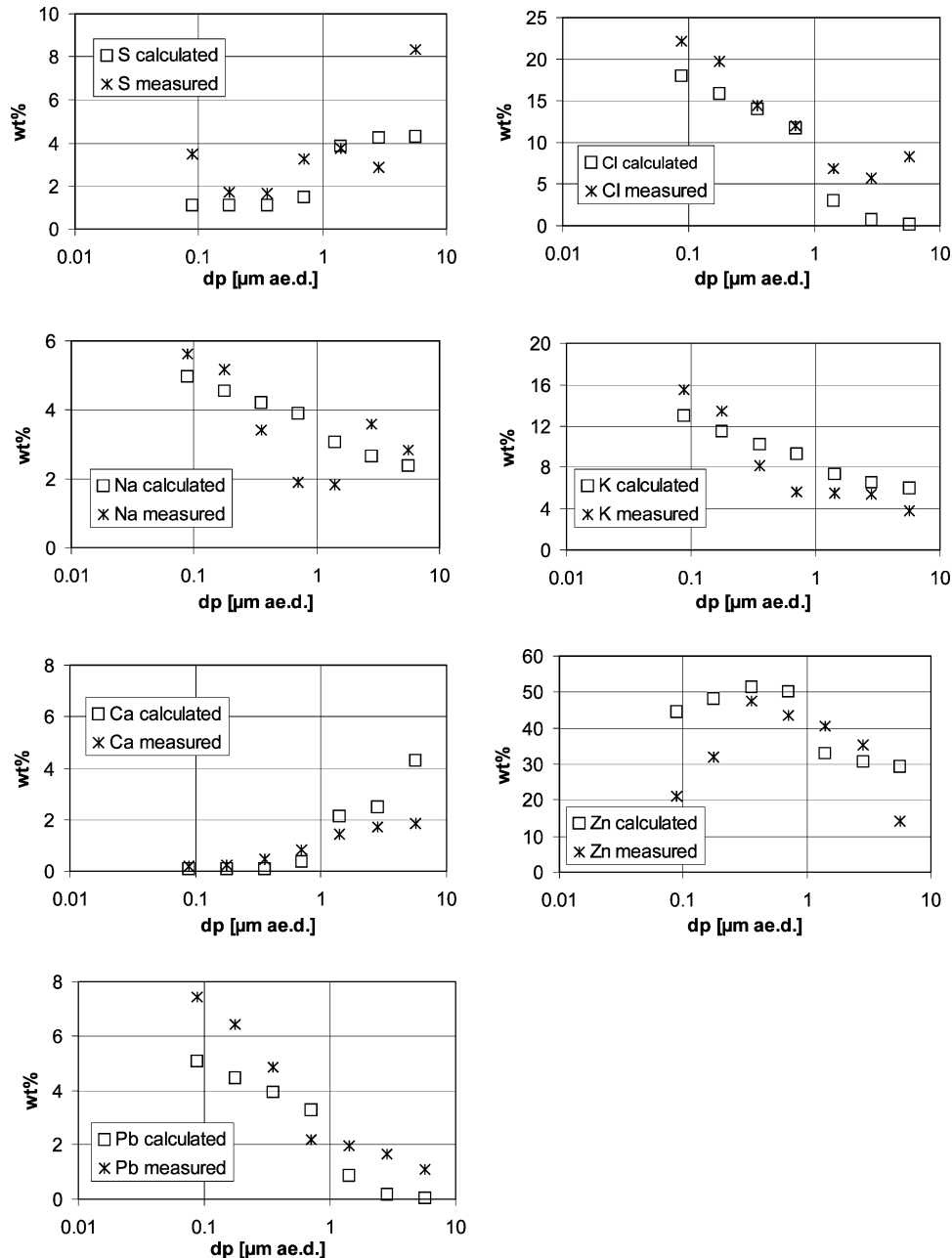


Figure 12. Comparison of simulated and measured concentrations of aerosol forming compounds sampled on impactor plates at the boiler outlet during waste wood combustion; ae.d., aerodynamic diameter.

Test runs at a 440 kW_{th} pilot plant were performed for the calibration and testing of the model. The operating data of these test runs and fuel and ash analyses provided the basis for mass balances for the relevant aerosol-forming species in order to obtain all elemental concentrations of particles and flue gas leaving the fuel bed. Furthermore, BLPI measurements were performed and the particles subsequently analyzed in order to determine the mean aerosol particle size distributions and compositions of aerosols at the boiler outlet. The operating data and element release data were then used to simulate the formation of aerosol particles from the combustion of the two investigated fuels.

Good agreement between the calculated and the measured particle size distributions was observed. The main peak was located on the same impactor stages for calculated and measured PSDs. Furthermore, the total mass of aerosols was in the same order of magnitude

but a little lower for the calculated PSDs. This slight underprediction of the aerosol mass concentration at the boiler outlet might be due to the simplification of the plug flow model and the missing implementation of a particle-deposit erosion approach.

The amount and size of primary particles were predefined from the released ash forming matter. The location of the peak of submicron primary particles, which was found to be best situated around 0.02 and 0.08 μm for beech and waste wood, respectively, had a considerable influence on the resulting PSD; the composition of the primary particles was determined by thermodynamic equilibrium calculations, which showed CaO, MgO, SiO₂, ZnO, and partially CaSO₄, K₂SO₄, and Na₂SO₄ to be stable at temperatures between 900 and 1200 °C. In regard to the gas composition, SO_x emissions were well-predicted by adapting the kinetic limitation of SO₂ oxidation to the Arrhenius expression as de-

scribed above, but HCl emissions, which were not considered as kinetically limited, were too low.

The composition of the aerosol fractions was reproducible especially for major aerosol-forming elements in the aerosol fractions. The prediction of concentrations of the coarse particle composition was strongly dependent on the predefined primary particles and showed poor compliance, probably due to averaged composition assumptions and the treatment of the coarse particles as spheres. Additionally, possible fluctuations of the flue gas composition and subsequent impacts on the measured aerosol composition as well as the small amount of mass sampled from coarse particles on impactor stages may cause divergences.

In conclusion, it can be stated that the model is applicable for a simplified simulation of aerosol formation during biomass combustion. Aerosol mass and composition can be predicted well, and the influences of combustion unit and fuel composition can be considered in detail. The model is a good basis for further work, which should include the determination of size and composition of primary particles and the development of an improved deposit formation model.

Acknowledgment. The authors thank the Institute of Electron Microscopy at Graz University of Technology for the good cooperation.

Nomenclature

A_{pr} [-] = coefficient for calculation of precipitation efficiency
 C_{FS} [-] = Fuchs-Sutugin correction factor

d_{50} [m] = cut diameter of an impactor stage
 d_p, d_{pj} [m] = particle diameter (of size class j)
 d_t [m] = tube diameter
 D_i [m²/s] = diffusion coefficient of gas component i
 $D_{p,j}$ [m²/s] = particle diffusion coefficient of size class j
 $F_{i,j}$ [mol/m³] = rate of condensation on particle surfaces
 I [m⁻³s⁻¹] = nucleation rate
 K_{th} [-] = thermophoretic factor
 l [m] = tube length
 N, N_0 [m⁻³] = number concentration, initial number concentration
 N_j [m⁻³] = number of particles of size class j
 p_i [Pa] = vapor pressure of component i
 $p_{i,S}$ [Pa] = saturation vapor pressure of component i
 r^* [m] = critical droplet radius
 R_{gas} [J/(mol K)] = universal gas constant
 Re, Re_p [-] = Reynolds number of gas stream and particle
 t [s] = time
 T [K] = temperature
 v_p, v_{dep} [m/s] = particle velocity, particle deposition velocity
 v_{gas} [m/s] = gas velocity

Greek Letters

η_{gas} [kg/(ms)] = dynamic viscosity of the flue gas
 η_{pr} [-] = precipitation efficiency
 ρ_{gas} [kg/m³] = gas density
 τ [m] = Tolman length

EF049904M